IOP PUBLISHING JOURNAL OF PHYSICS D: APPLIED PHYSICS

J. Phys. D: Appl. Phys. **43** (2010) 245101 (5pp) doi:10.1088/0022-3727/43/24/245101

Improvement of efficiency in solar cells based on vertically grown copper phthalocyanine nanorods

S Karak, S K Ray and A Dhar[1]

Department of Physics and Meteorology, Indian Institute of Technology Kharagpur, Kharagpur-721 302, India

E-mail: adhar@phy.iitkgp.ernet.in

Received 8 February 2010, in final form 27 April 2010
Published 1 June 2010
Online at stacks.iop.org/JPhysD/43/245101

Abstract

We have fabricated efficient organic photovoltaic cells using copper phthalocyanine (CuPc) nanorods as donor and [6,6]-phenyl C_{61} butyric acid methyl ester (PCBM) as the acceptor material. Highly dense randomly oriented and vertically aligned nanorods with diameters of about 30–50 nm have been achieved from vacuum-deposited CuPc films by simple surface solvent treatment. X-ray diffraction confirms the polycrystalline nature of the CuPc nanorods. Significantly improved cell performance was observed with the change in shape and orientations of the nanorods. Maximum power conversion efficiency of 2.57% was obtained from the vertically aligned nanorods, which is a result of an increment in the donor–acceptor interface area and efficient photogenerated charge carrier transports.

(Some figures in this article are in colour only in the electronic version)

1. Introduction

In recent decades, organic photovoltaic devices (OPVs) have opened up a promising route for renewable solar energy because of their low-cost potential, lightweight, mechanical flexibility and ease of processing. Since Tang proposed the first efficient bilayer organic solar cell [1], a significant effort has been made to improve the device performance [2–6]. However, the power conversion efficiency (η) of OPVs is still lower than that of inorganic or dye-sensitized solar cells because of the short exciton diffusion length of organic semiconductors [7]. Currently, donor/acceptor (D/A) bulk heterojunctions with large D/A interface have been widely used to overcome such an exciton diffusion bottleneck [8–10]. Still, the random interpenetrating D/A network could lead to charge trapping and poor charge carrier transport due to the non-uniform phase separation within the D/A mixture and formation of structural islands or cul-de-sacs along the conducting paths [11, 12]. Therefore, bulk heterojunction with controlled nanostructures which ensure a large D/A interface for efficient exciton dissociation as well as a continuous conducting path for rapid charge carrier transport is essential for further improvement. To date, such controlled nanostructure based organic solar cells have rarely been investigated [11, 13–15].

In this paper, we report on the photovoltaic properties of copper phthalocyanine (CuPc) nanorod based efficient organic solar cells. Overall cell performance is found to be strongly dependent on the shape and orientation of the nanorods. A maximum power conversion efficiency of (η) 2.57% and an external quantum efficiency (EQE) of around ~42% have been achieved from the devices containing arrays of vertical CuPc nanorods of 40–60 nm diameters.

2. Experimental

The photovoltaic devices were fabricated on pre-cleaned patterned indium tin oxide (ITO) coated (sheet resistance ~10 Ω/□) glass substrates. Prior to any active layer deposition, a 40 nm thick poly(3,4-ethylenedioxythiophene)-poly(styrenesulfonate) (PEDOT : PSS) layer (2.8 wt% water solution) was spin coated on ITO anodes and dried at around 110 °C for 1 h. A 50 nm thick CuPc (99%) layer was then thermally evaporated on top of the PEDOT : PSS layer. The nanostructures were grown using a simple solvent

[1] Author to whom any correspondence should be addressed.

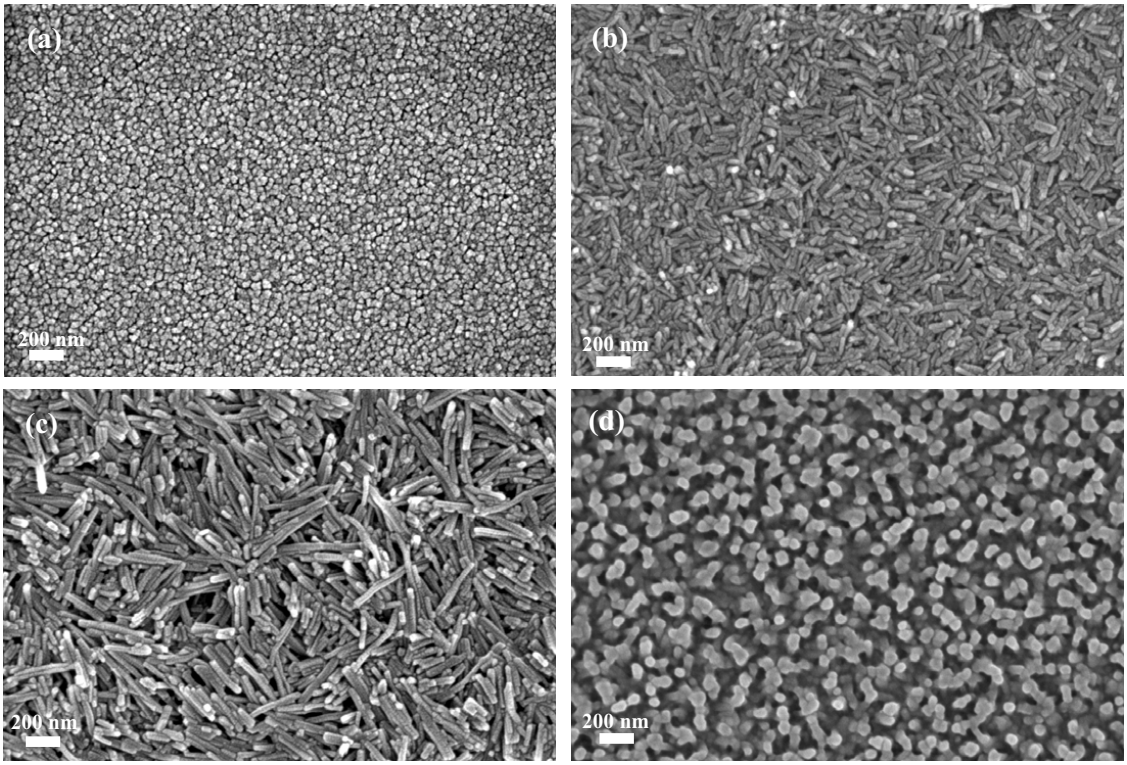

Figure 1. FESEM images of the CuPc films: (*a*) as deposited (R_1); (*b*) treated with chlorobenzene (R_2); (*c*) treated with toluene (R_3) and (*d*) acetone treated (R_4).

treatment process by dropping different solvents (such as chlorobenzene, toluene and acetone) on the surface of the CuPc film [16]. A [6,6]-phenyl C_{61} butyric acid methyl ester (PCBM, 99%) layer was deposited by spin-coating using a solution in chlorobenzene (20 mg ml^{-1}). The CuPc/PCBM composite films were then annealed at 80 °C for 30 min to remove the residual solvent completely followed by the deposition of a 10 nm thick electron transporting layer (ETL) of bathocuproine (BCP, 99%). Finally, an 80 nm thick aluminium top electrode strip was deposited by thermal evaporation through a shadow mask to define a square shaped active area of 4 mm^2. Base pressure during the thermal evaporation was 5×10^{-6} mbar. Quartz crystal monitor and stylus profilometer (Veeco Dektak3) were used to monitor and to verify the thickness of the different layers. Scanning electron microscope with field-emission cathode (FESEM) images of the different types of CuPc nanorods were taken using a ZEISS SUPRA 40 field emission (FE) microscope, and a Philips X-Pert PRO MRD x-ray diffractometer with Cu Kα radiation ($\lambda = 0.154\,18$ nm) was used to investigate the crystallinity of the nanorods. The absorption spectra of the CuPc/PCBM heterojunctions were investigated using a UV–VIS–NIR spectrophotometer (Perkin-Elmer Lambda 45). A Keithley 4200-SCS measurement unit together with a Newport 67005 solar simulator were used to measure the current density–voltage (J–V) characteristics of the devices under dark and AM 1.5 (100 mW cm^{-2}) simulated solar irradiation conditions. For the photocurrent action spectrum measurements at short-circuit condition, a lock-in amplifier (Standford research system-SR830 DSP) was used with a chopping frequency of 180 Hz during illumination of the samples with monochromatic light from a broad band source and the photoluminescence (PL) lifetime decay measurements were done using an Edinburgh Instruments (Life Spec-II, EPL 405) measurement unit with a 404.4 nm excitation pulse diode laser. All the device characterizations have been carried out under ambient conditions.

3. Results and discussion

CuPc molecules have been extensively used in a wide range of applications in the field of organic electronics for their outstanding electrical and optical properties. So far, the most efficient small molecule PV device has been fabricated using CuPc as the donor material [3, 17] and for further improvement tailoring is required at the nanostructure level. Here we have fabricated CuPc nanorods of different shapes, sizes and orientations using different solvent treatments from a vacuum-deposited 50 nm thick CuPc film [16]. For this, we added different solvents (such as chlorobenzene, toluene and acetone) on the surface of the as deposited CuPc film and allowed the solvent to evaporate at room temperature. While the solvent volatilized completely, different nanostructures were formed for different solvent after recrystallization of the CuPc film. Nanorods of various shapes, sizes and orientations were produced for different solvents because of their different solubilities, polarities and boiling points, which lead to different interactions with the CuPc molecules. Figure 1(*a*) shows the FESEM image of the as deposited CuPc film (labelled as R1) with relatively flat surface morphology whereas figures 1(*b*), (*c*) and (*d*) show the films treated with

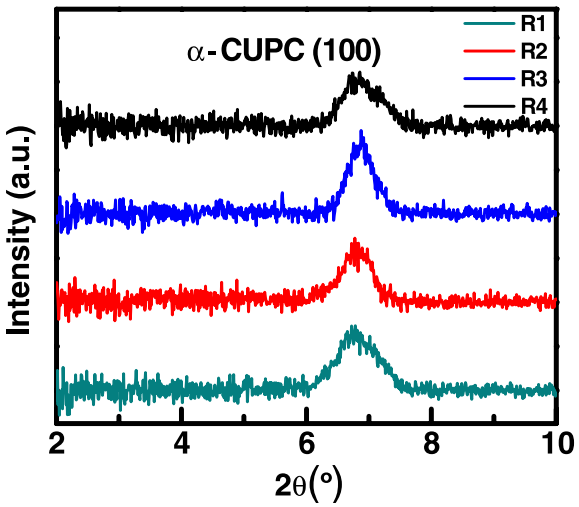

Figure 2. XRD patterns of different solvent treated CuPc films grown on glass/ITO/PEDOT : PSS substrates.

chlorobenzene, toluene and acetone, respectively (henceforth, labelled as R2, R3 and R4, respectively), with substantial changes in nanostructures. Films treated with chlorobenzene showed randomly oriented small nanorods with diameters of about 15–35 nm and lengths of about 100–200 nm whereas for the films treated with toluene, comparatively large randomly oriented nanorods with diameters of about 30–50 nm and lengths of about 200–400 nm were obtained. Interestingly, acetone treated films showed completely different highly dense standing nanorods with diameters of around 40–60 nm. It is quite interesting that the dimensions of all these nanostructures are comparable to the exciton diffusion length of CuPc [7, 18] and hence they can significantly enhance the photocarrier generation of the devices. The x-ray diffraction (XRD) patterns of the as deposited CuPc film along with the different solvent treated films are shown in figure 2. The diffraction peak at $2\theta = 6.9^\circ$ confirms the existence of the polycrystalline α-CuPc phase for the nanorods as well as for the untreated film [19–21] which ensures that the short-time solvent treatment did not destroy the polycrystalline nature and the stacking pattern of the CuPc molecules. This is important for efficient hole transport through the nanorods and high collection efficiency for photogenerated holes in the PV devices.

Figure 3(a) shows the current density–voltage (J–V) characteristics of the cells under dark condition. All the devices exhibit rectifying diode characteristics as expected from heterojunction devices sandwiched between electrodes having different work functions. The overall shape of the J–V curve under forward bias of the devices does not change considerably, suggesting that there is no significant modification of band structures at the interfaces with a change in shapes, size and orientation of the nanorods. On the other hand, reverse bias current remains almost the same for the untreated (R1), chlorobenzene treated (R2) and acetone treated (R4) samples with a rectification ratio of $\sim 10^3$ (at ± 1 V) whereas the toluene treated sample (R3) showed relatively higher leakage current with a rectification ratio of $\sim 4 \times 10^2$. This is mainly due to the shadow effect of the randomly

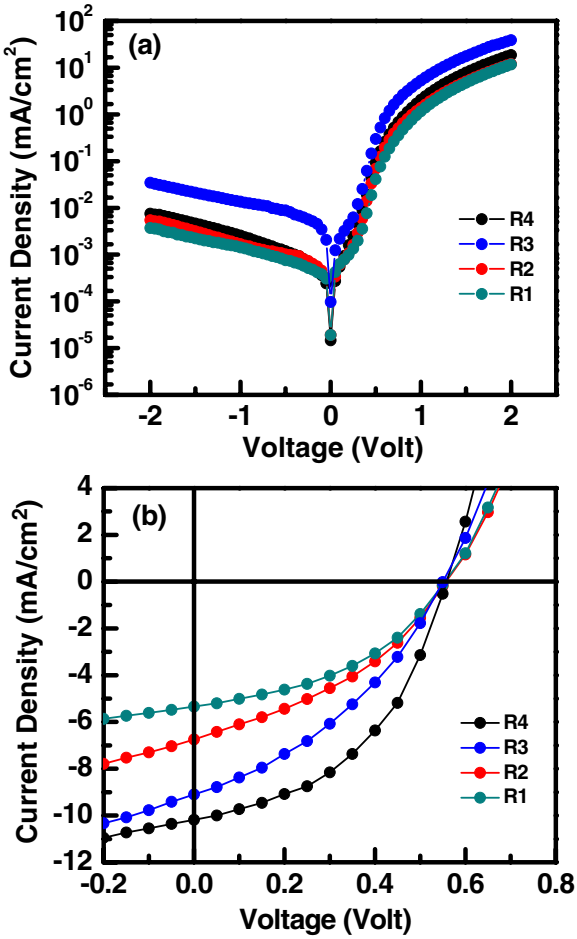

Figure 3. (a) Dark J–V curves for the as deposited and for the different solvent treated samples. (b) J–V characteristics of the devices under 100 mW cm^{-2} AM 1.5 simulated solar irradiation conditions.

oriented nanostructures, leading to the partial infiltration of PCBM into the spacing between the nanorods and creating pin-holes and microscopic shorts within the devices which ultimately decrease the shunt resistance. Figure 3(b) shows the J–V characteristics of all the devices under 100 mW cm^{-2} AM 1.5 simulated solar irradiation condition. The untreated samples (R1) exhibit a short-circuit current density (J_{SC}) of 5.34 mA cm^{-2}, an open-circuit voltage (V_{OC}) of 0.55 V and a fill factor (FF) of 43.1% which lead to a power conversion efficiency (η) of 1.25% whereas the chlorobenzene treated sample (R2) showed a η of 1.42% with a J_{SC} of 6.74 mA cm^{-2} and FF of 38.4%, toluene treated samples (R3) showed a η of 1.83% with a J_{SC} of 9.1 mA cm^{-2} and FF of 36.6% and acetone treated samples showed a η of 2.57% with a J_{SC} of 10.18 mA cm^{-2} and FF of 46.1%. V_{OC} remains unchanged for all the devices as it depends mostly upon the energy gap between the highest occupied molecular orbital (HOMO) level of donor material and the lowest unoccupied molecular orbital (LUMO) level of the acceptor material. FF of the R3 devices is comparatively low because of the pin-holes and microscopic shorts within the devices resulting from the poor infiltration of the PCBM layer. Interestingly, improvement in the power conversion efficiency of the cells is mainly

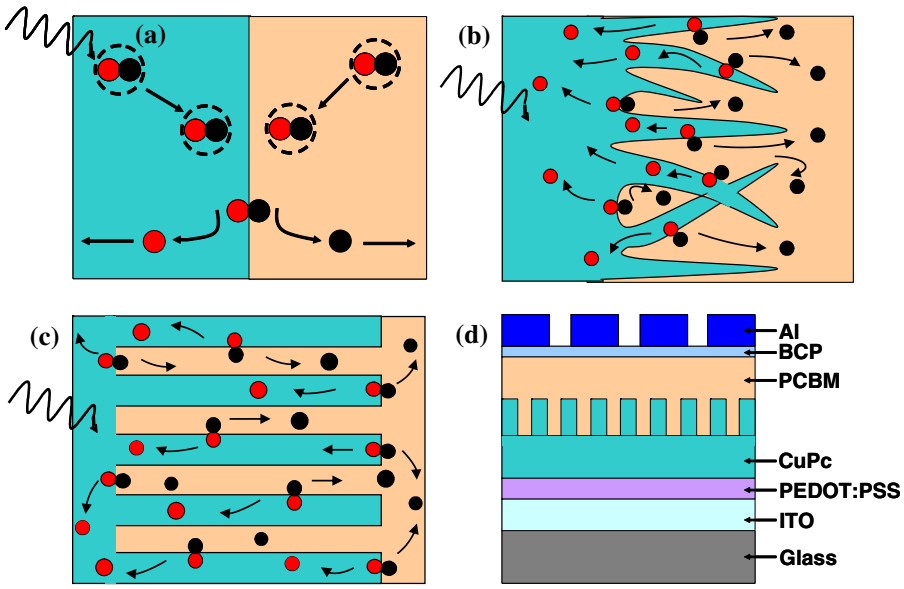

Figure 4. Schematic diagram of the photocarrier generation for the (*a*) planar heterojunction, (*b*) randomly oriented nanorod based heterojunction, (*c*) the controlled growth standing nanorod based heterojunction with large D/A interface area and (*d*) schematic diagram of the photovoltaic devices with vertically aligned CuPc nanorods.

due to the enhancement in the J_{SC}. With the change in the orientation of the CuPc nanostructures, the effective D/A interface area increases, leading to a higher probability of exciton dissociation and thereby increasing the J_{SC}. The schematic diagram of the photocarrier generation for the different nanostructures and the complete device structure are shown in figure 4.

The inset of figure 5(*a*) represents the absorption spectra and figure 5(*a*) shows the photocurrent action spectra of the devices, which closely follows the absorption profile of the CuPc/PCBM heterojunction. The EQE was measured using the relation

$$\mathrm{EQE}(\%) = \left(\frac{100 \times 1240 \times J_{sc}}{\lambda P_0}\right), \qquad (1)$$

where P_0 is the incident light intensity of the source (mW cm^{-2}), J_{SC} is the short-circuit current density (mA cm^{-2}) and λ is the wavelength (nm) of incident radiation. Untreated samples showed an EQE of ∼15% whereas it improves to ∼18% and ∼31% for the chlorobenzene and toluene treated samples, respectively. The maximum EQE of ∼42% at 624 nm is obtained for the samples treated with acetone, which is almost three times greater than the untreated one. Such a significant improvement in the EQE indicates efficient exciton dissociation as well as improved charge collection for nanostructure based devices.

In order to get more insight into the photo-physics of the devices, we perform time resolved PL experiment at a wavelength of 520 nm, for all the samples as shown in figure 5(*b*). It is found that the PL lifetime (∼1.66 ns) for the vertical nanorod based devices is significantly lower than the untreated one (∼4.31 ns), indicating more efficient charge separation at the interfaces between nanorods and the PCBM layer than the planar heterojunction. Chlorobenzene

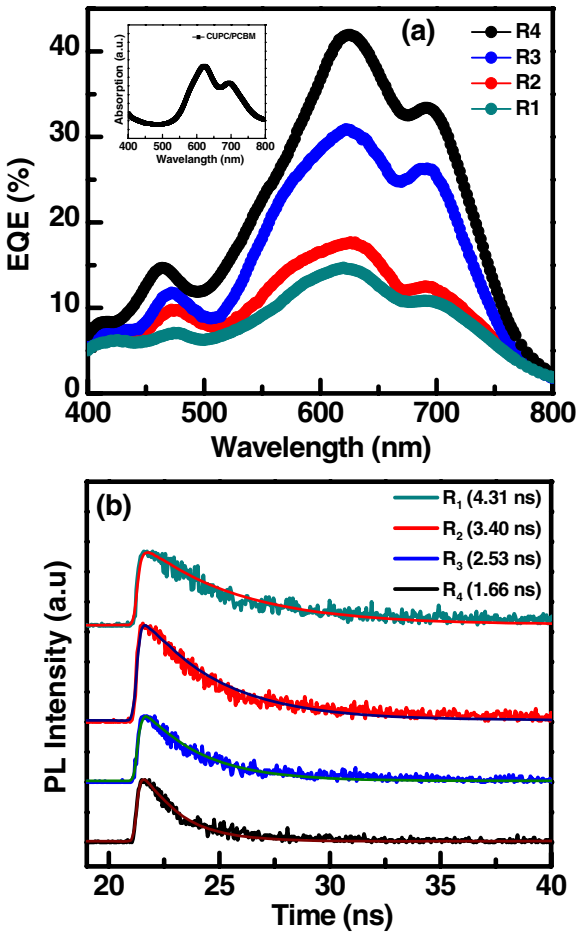

Figure 5. (*a*) Photocurrent action spectra of the devices treated with different solvents. Inset: absorption spectrum of the CuPc/PCBM heterojunction. (*b*) PL lifetime decay of different solvent treated CuPc/PCBM heterojunctions.

(∼3.40 ns) and toluene (∼2.53 ns) treated samples also showed relatively lower PL lifetime. This reveals that the nanostructures are forming more favourable interfaces for efficient exciton dissociation compared with the conventional bilayer heterojunctions.

4. Conclusion

To conclude, we have investigated the photovoltaic properties of CuPc nanostructure based OPVs. Strong dependences of overall cell performances were observed with the change in shape, size and orientation of the nanostructures. Maximum η of 2.57% have been achieved for the cells containing arrays of vertical nanorods, which is almost double compared with the untreated CuPc/PCBM heterojunction solar cell. This improvement is mainly due to the increase in the effective D/A interface area. With further optimization of the nanostructures and the device fabrication processes, further improvement in the efficiency of OPVs is expected using this architecture.

Acknowledgments

One of the authors (S Karak) acknowledges CSIR, Govt of India, for the award of a Junior Research Fellowship.

References

[1] Tang C W 1986 *Appl. Phys. Lett.* **48** 183
[2] Shaheen S E, Brabec C J, Sariciftci N S, Padinger F, Fromherz T and Hummelen J C 2001 *Appl. Phys. Lett.* **78** 841
[3] Peumans P and Forrest S R 2001 *Appl. Phys. Lett.* **79** 126
[4] Li G, Shrotriya V, Huang J S, Yao Y, Moriarty T, Emery K and Yang Y 2005 *Nature Mater.* **4** 864
[5] Xue J G, Uchida S R, B P and Forrest S R 2004 *Appl. Phys. Lett.* **85** 5757
[6] Kim J Y, Lee K, Coates N E, Moses D, Naguyen T Q, Dante M and Hegger A J 2007 *Science* **317** 222
[7] Peumans P, Yakimov A and Forrest S R 2003 *J. Appl. Phys.* **93** 3693
[8] Halls J J M, Walsh C A, Greenham N C, Marseglia E A, Friend R H, Moratti S C and Holmes A B 1995 *Nature* **376** 498
[9] Yu G, Gao J, Hummelen J C, Wudl F and Heeger A J 1995 *Science* **270** 1789
[10] Peumans P, Uchida S and Forrest S R 2003 *Nature* **425** 158
[11] Yang F, Shtein M and Forrest S R 2005 *Nature Mater.* **4** 37
[12] Sun S, Fan Z, Wang Y and Haliburton J 2005 *J. Mater. Sci.* **40** 1429
[13] Dissanayake D M N M, Adikaari A A D T, Curry R J, Hatton R A and Silva S R P 2007 *Appl. Phys. Lett.* **90** 253502
[14] Castro F A, Benmansour H, Graeff C F O, Nesch F, Tutis E and Hany R 2006 *Chem. Mater.* **18** 5504
[15] Orozco M C, Tsoi W C, O'Neill M, Aldred M P, Vlachos P and Kelly S M 2006 *Adv. Mater.* **18** 1754
[16] Xi H, Wei Z, Duan Z, Xu W and Zhu D 2008 *J. Phys. Chem.* C **112** 19934
[17] Xue J G, Uchida S R and B P and Forrest S R 2004 *Appl. Phys. Lett.* **84** 3013
[18] Stubinger T and Brutting W 2001 *J. Appl. Phys.* **90** 3632
[19] Berger O, Fischer W J, Adolphi B, Tierbach S, Melev V and Schreiber J 2000 *J. Mater. Sci.: Mater. Electron.* **11** 331
[20] Prabakaran R, Kesavamoorthy R, Reddy G L N and Xavier F P 2002 *Phys. Status Solidi* b **229** 1175
[21] Xue J, Rand B P, Uchida S and Forrest S R 2005 *J. Appl. Phys.* **98** 124903